

To **boldly go** into a **new dimension**: 3D raypath interferometry

David C. Henley*
dhenley@ucalgary.ca]

• SUMMARY

Raypath interferometry corrects seismic reflection data for near-surface effects in a **nonstationary** and **wavefront-consistent** manner, in order to properly handle S-wave data, as well as difficult PP data. We extend it here to **3D** and discover **problems**.

• PRINCIPLES of the method

Nonstationarity and **wavefront-consistency** are introduced:

• **Surface-consistency** replaced by **Raypath-consistency**

• **Time shifting** replaced by **surface function deconvolution**

• GEOMETRY for 3D

Seismic data, transformed to a '**common-raypath**' domain via a **2D transform** (Radial Trace or Tau-P), can be used for either 2D or 3D data as long as:

• **2D Surface function** extended to **3D**, with **azimuth** as the **3rd dimension** (Figure 1)

• **Approximately coplanar seismic trace ensembles** collected from the 3D dataset with **azimuth** as the **3rd dimension** (Figure 2)

• DEMONSTRATION on field data

The Blackfoot 3D 3C dataset was used to test and develop 3D raypath interferometry.

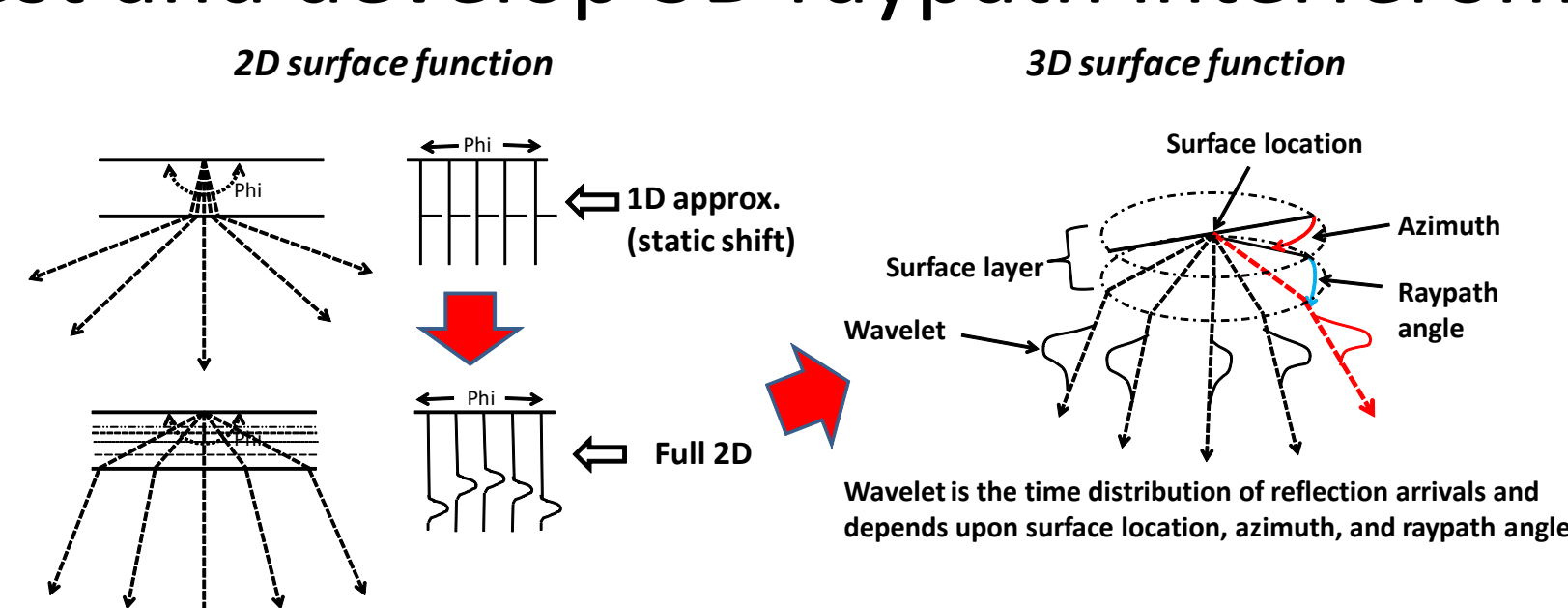


FIG. 1. Schematic showing 1D surface function (static shift) being extended to 2D when near-surface layer becomes more complex, then to 3D when azimuthal variation is included.

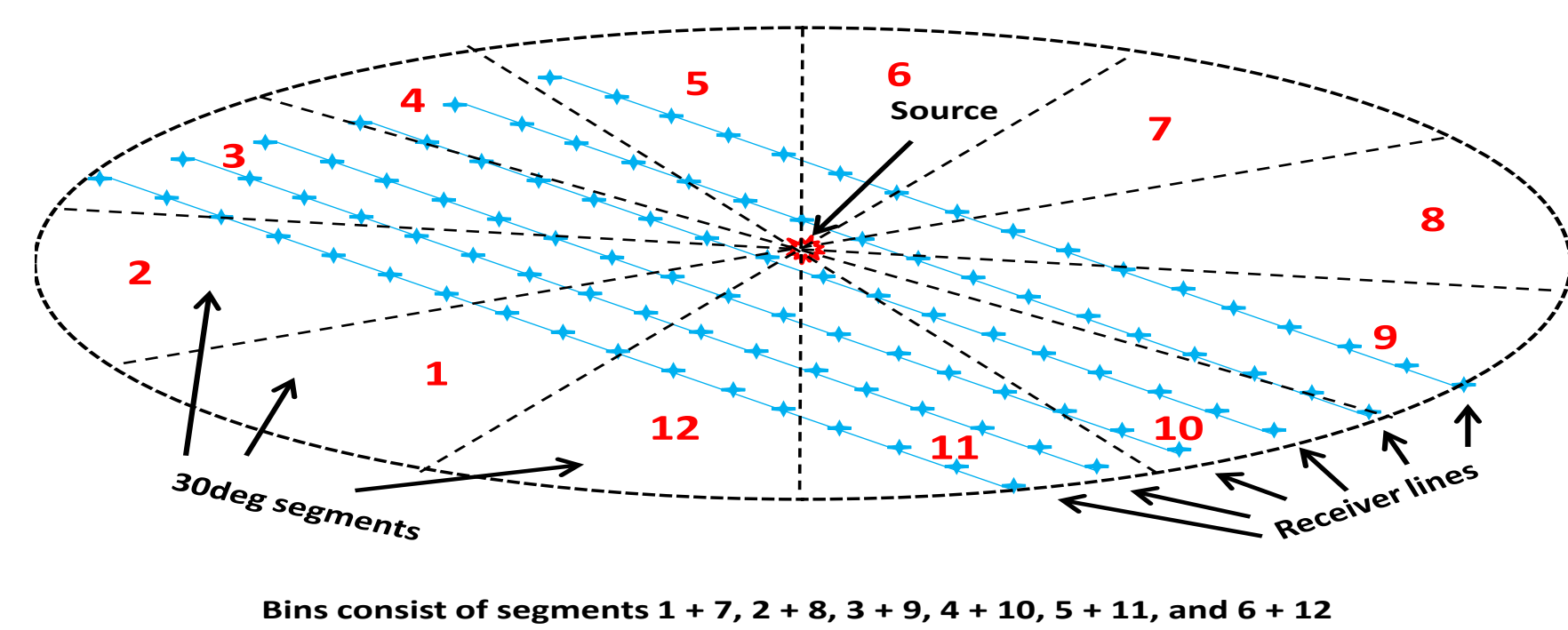


FIG. 2. Schematic showing how seismic traces recorded with conventional 3D geometry are collected into ensembles whose trace raypaths are roughly coplanar in the subsurface. The ensemble bins are propeller-shaped on the surface.

• RADIAL (PS) COMPONENT

In 2015, we introduced **azimuthal geometry** to apply raypath interferometry to vertical (PP) component data from the Blackfoot 3D 3C survey. In 2016, we began the more difficult PS component. Figure 3 shows a typical NMO-corrected source gather; Figure 4 shows the same gather sorted by azimuth and offset, ready for **2D raypath transform**.

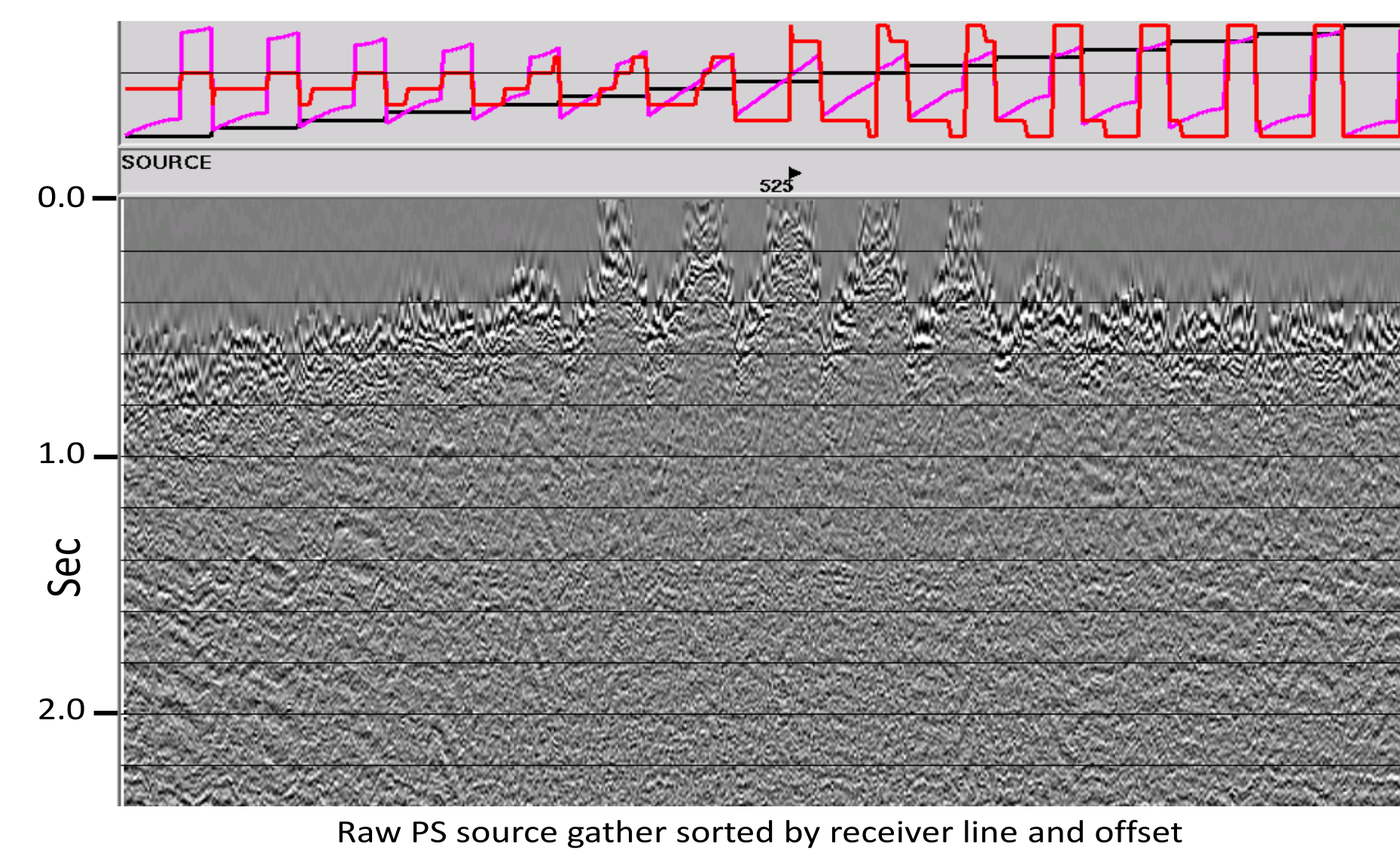


FIG. 3. Typical NMO-corrected radial component (PS) source gather, sorted by receiver line, from the Blackfoot 3D 3C data. Reflection/conversion events are not easily seen on this gather. (red=azimuth; pink=offset)

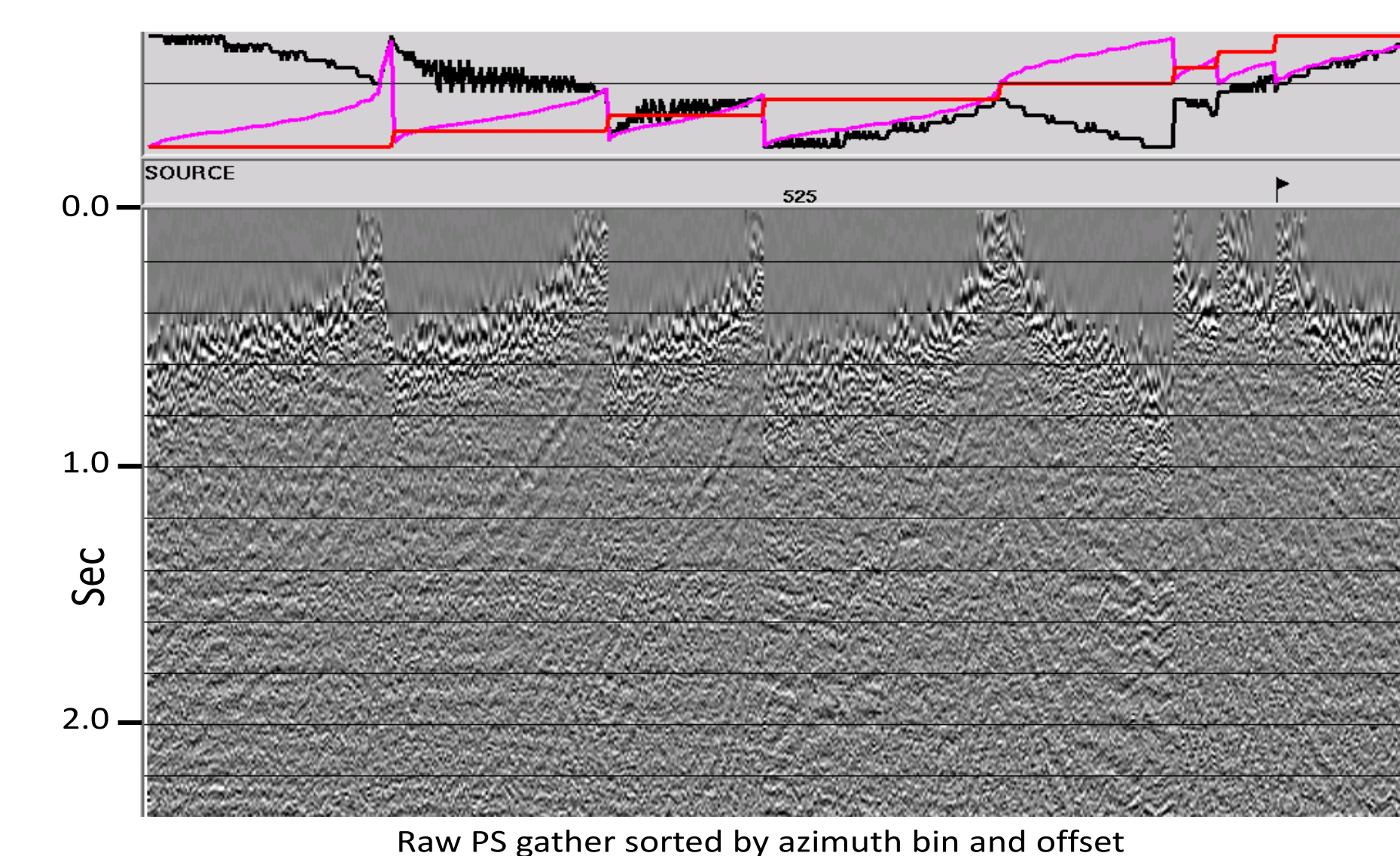


FIG. 4. Source gather of Figure 3, sorted by azimuth and offset. Events are much more coherent and easily seen in this ensemble, indicating that this is a good coordinate choice for analysis. (red=azimuth; pink=offset)

A **2D transform** (RT or Tau-P) is applied to each azimuth bin within a source ensemble. The traces are then sorted to common-ray-parameter ensembles. Figure 5 shows a **common-ray-parameter** ensemble **before interferometry**, Figure 6 shows the ensemble interleaved with the reference wavefield before cross-correlation, and Figure 7 shows the same common-ray-parameter ensemble **after interferometry**.

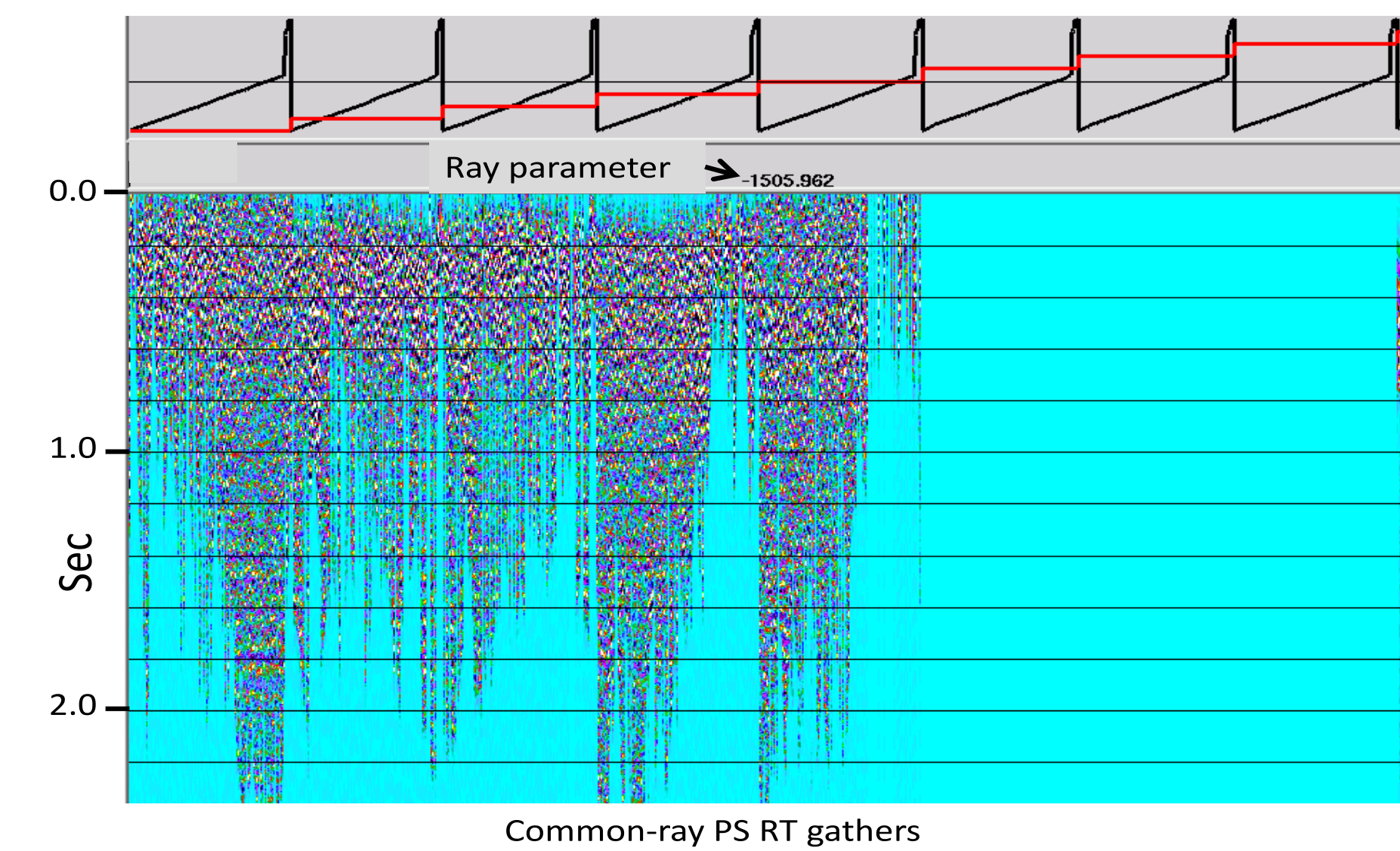


FIG. 5. Typical common-ray-parameter ensemble from Blackfoot radial component data. Very little event coherence can be seen at any time. (red=azimuth; black=source)

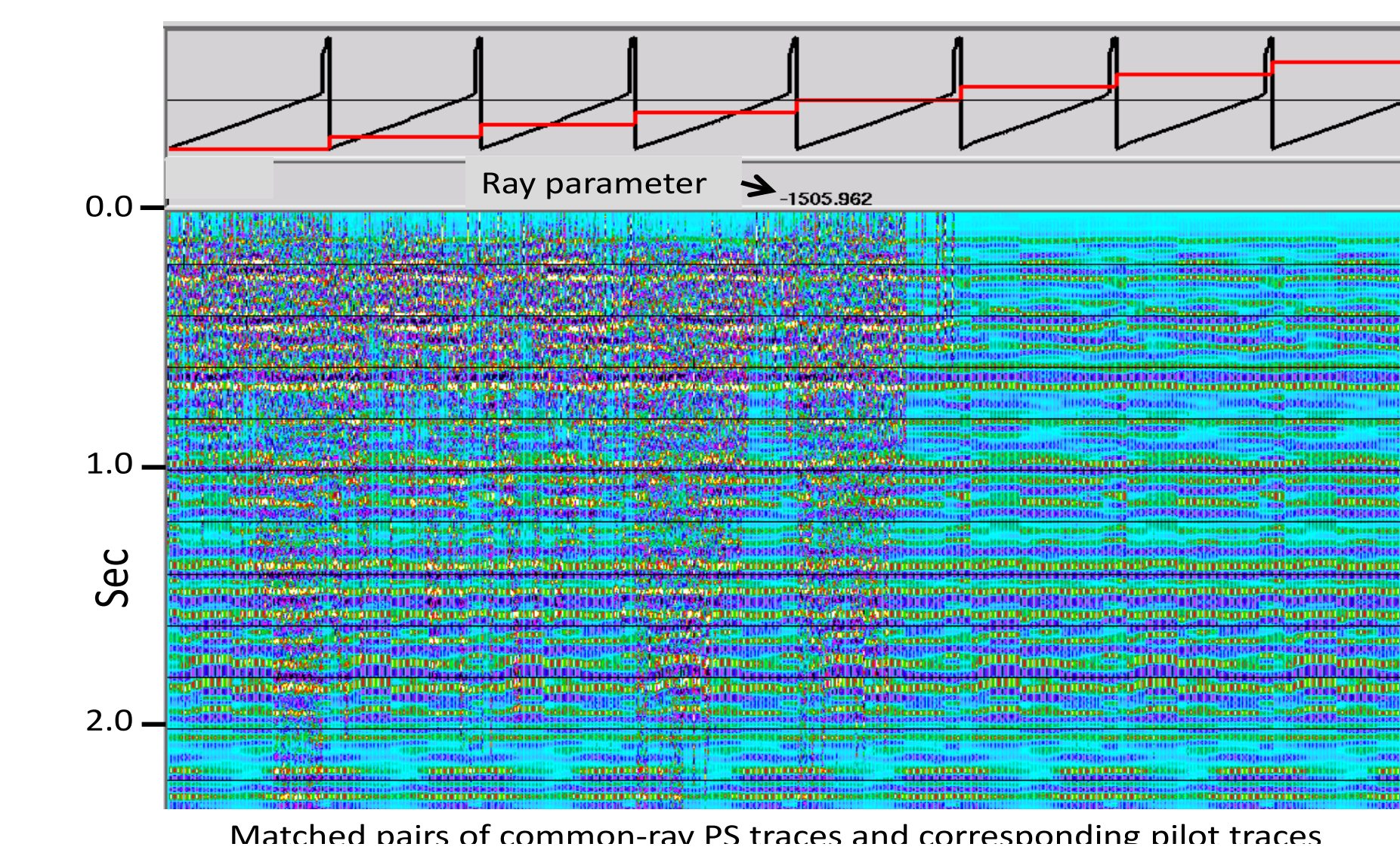


FIG. 6. Common-ray-parameter ensemble of Figure 5 interleaved with the 'reference wavefield' for this particular ray parameter. Pairwise cross-correlation creates 'surface functions', which are used to deconvolve the traces in Figure 5. (red=azimuth; black=source)

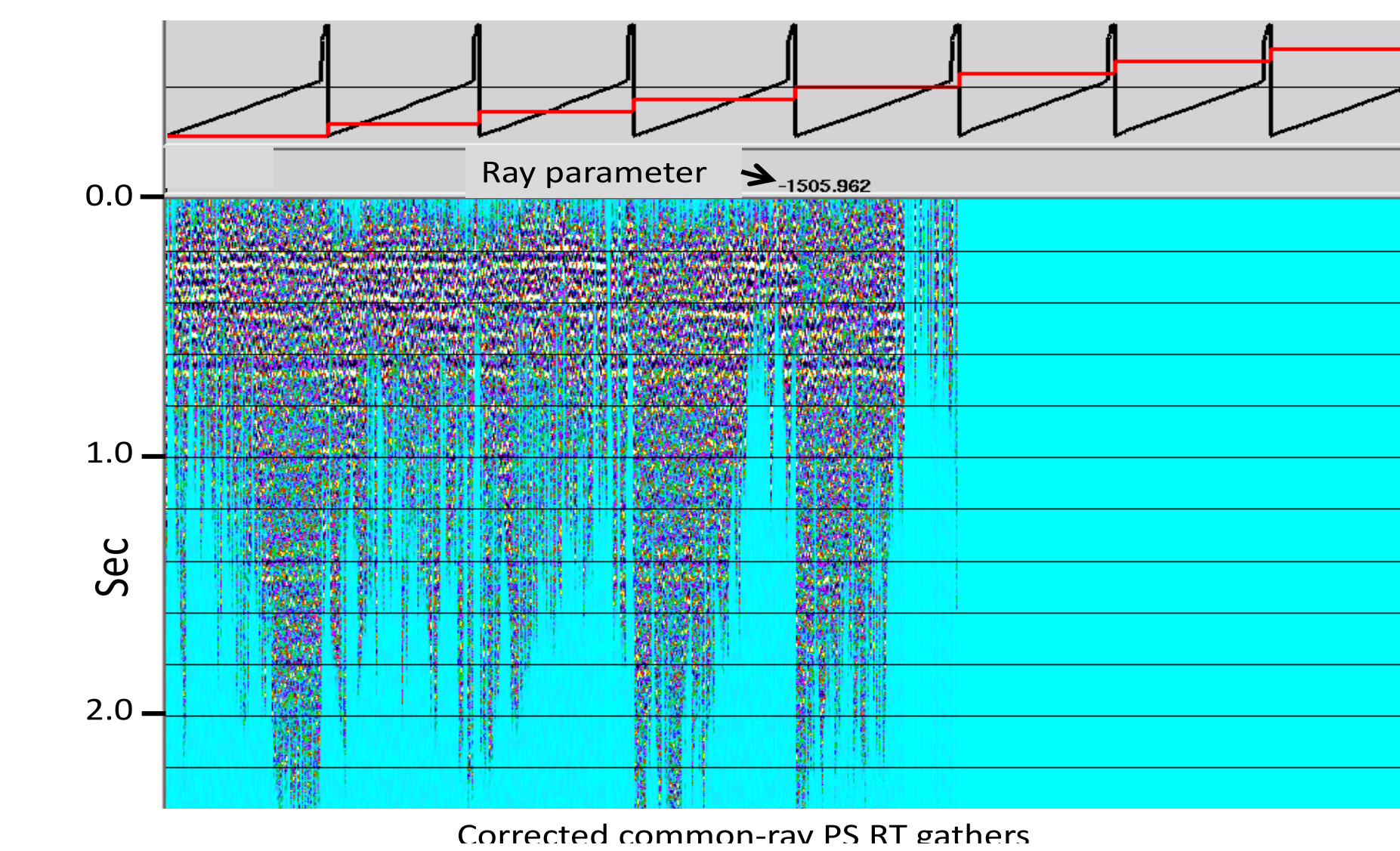


FIG. 7. Common-ray-parameter ensemble of Figure 5 after raypath interferometry. All events are now much more coherent, indicating successful removal of near-surface effects. (red=azimuth; black=source)

• PROBLEMS

The **main difficulty** for applying 3D raypath interferometry is the choice of **2D transform** used to move the data to the raypath domain and back:

- **Radial Trace (RT) Transform** does not restore **trace headers** properly in inverse.
- **Tau-P Transform** requires **massive storage** to apply with sufficient lateral resolution.

Figure 8 shows a PS **common-azimuth gather** with a **nonlinear offset distribution**, Figure 9 is the gather after forward/inverse **RT Transform**, and Figure 10 is the gather after forward/inverse **Tau-P Transform**. The Tau-P Transform requires **10 times the storage** (Figure 11), but fixing the **RT inverse** algorithm is **non-trivial**.

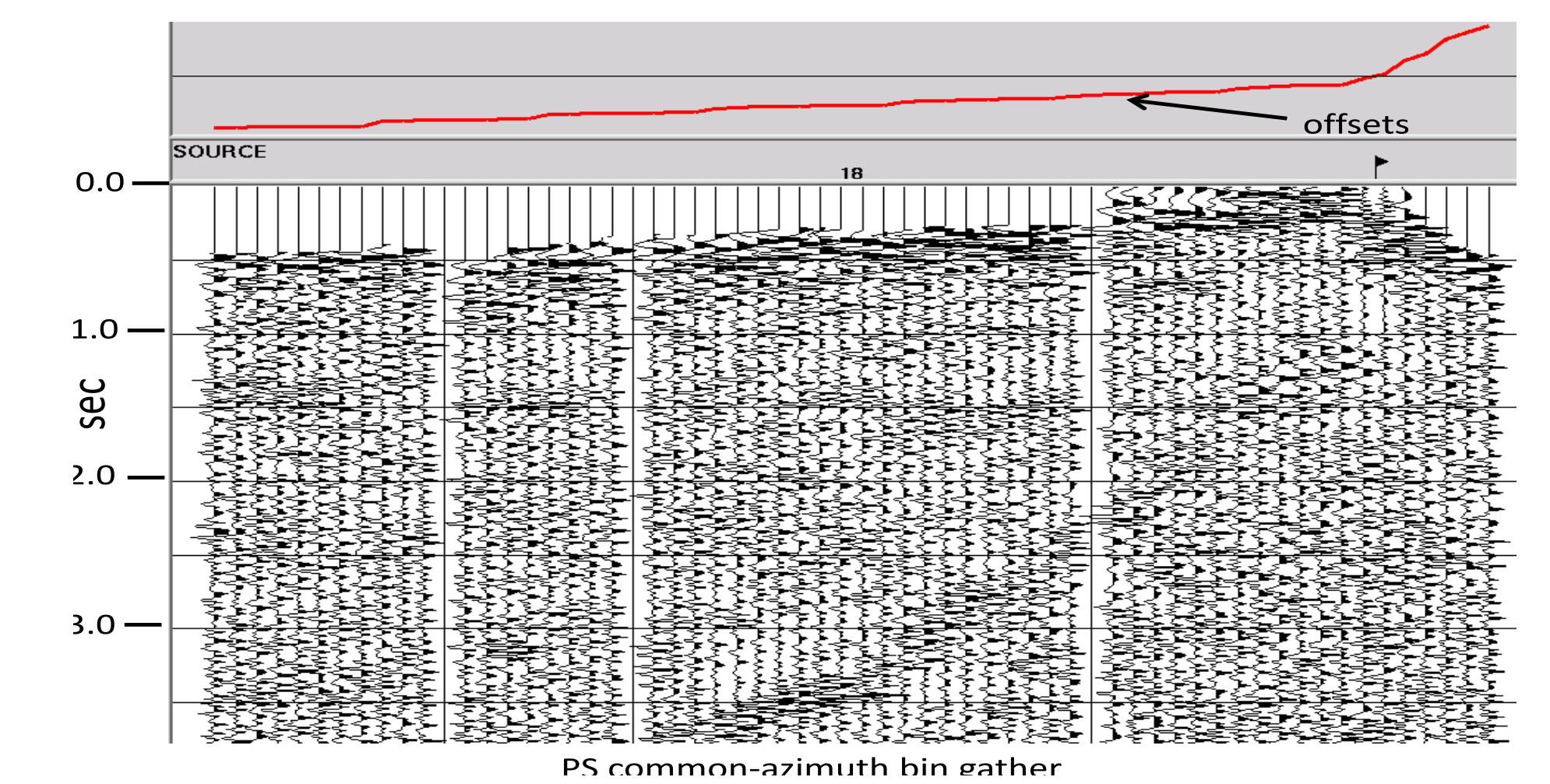


FIG. 8. Common-azimuth ensemble of PS traces with nonlinear distribution of source-receiver offset values.

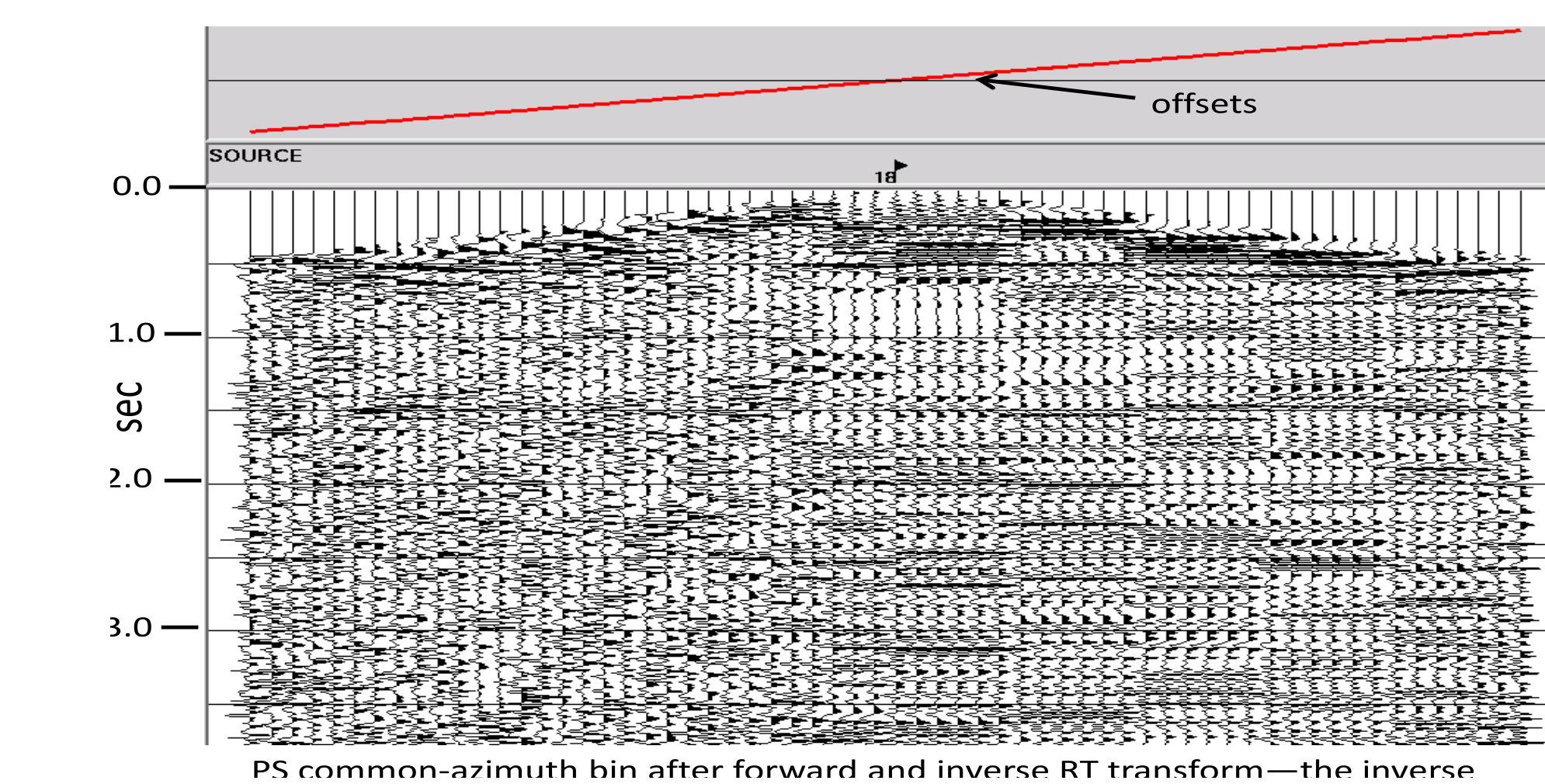


FIG. 9. Forward/inverse RT Transform of the ensemble in Figure 8. Data distortions are obvious, and not conducive to successful interferometry.

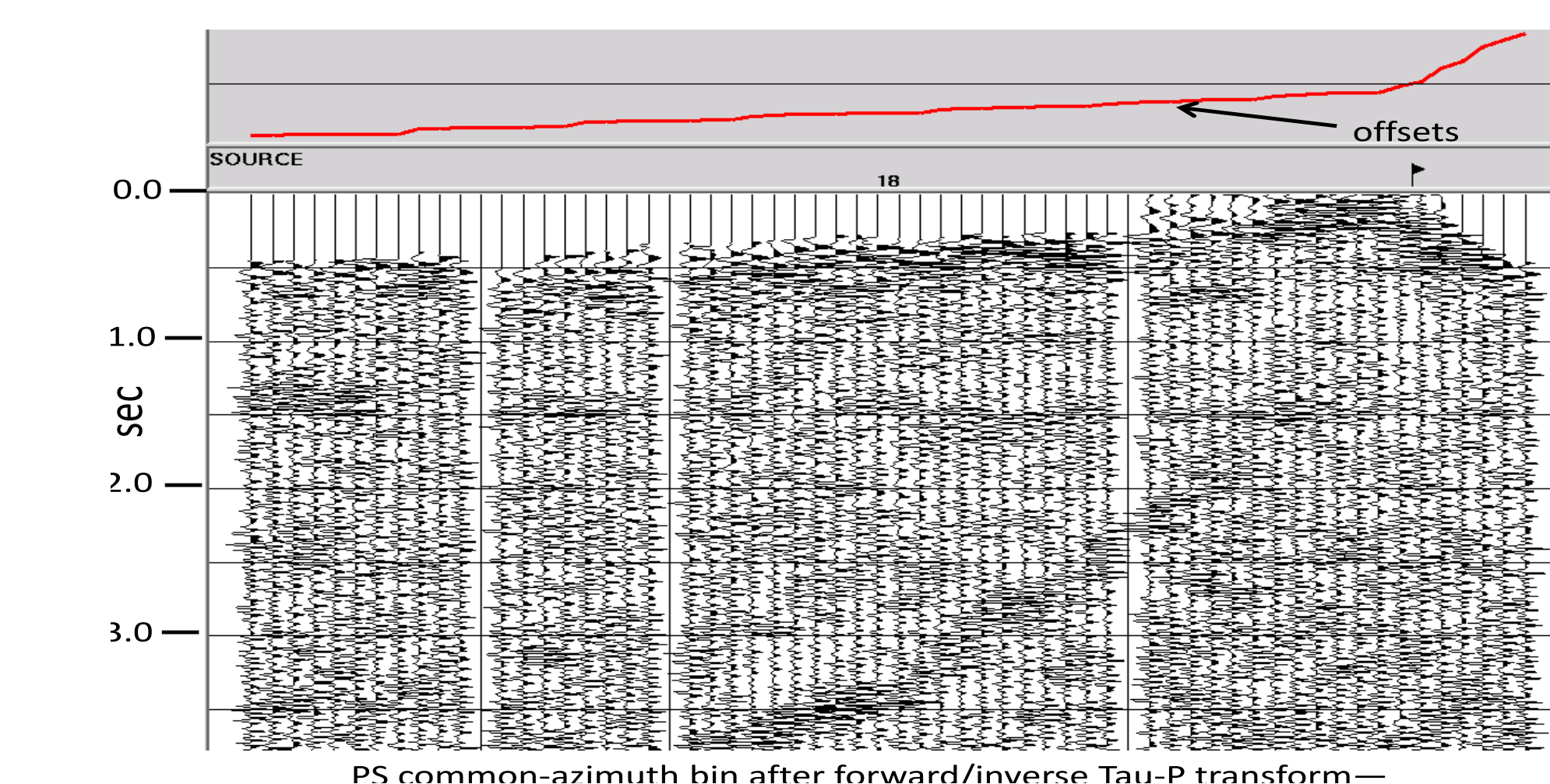


FIG. 10. Forward/inverse Tau-P transform of the ensemble in Figure 8.

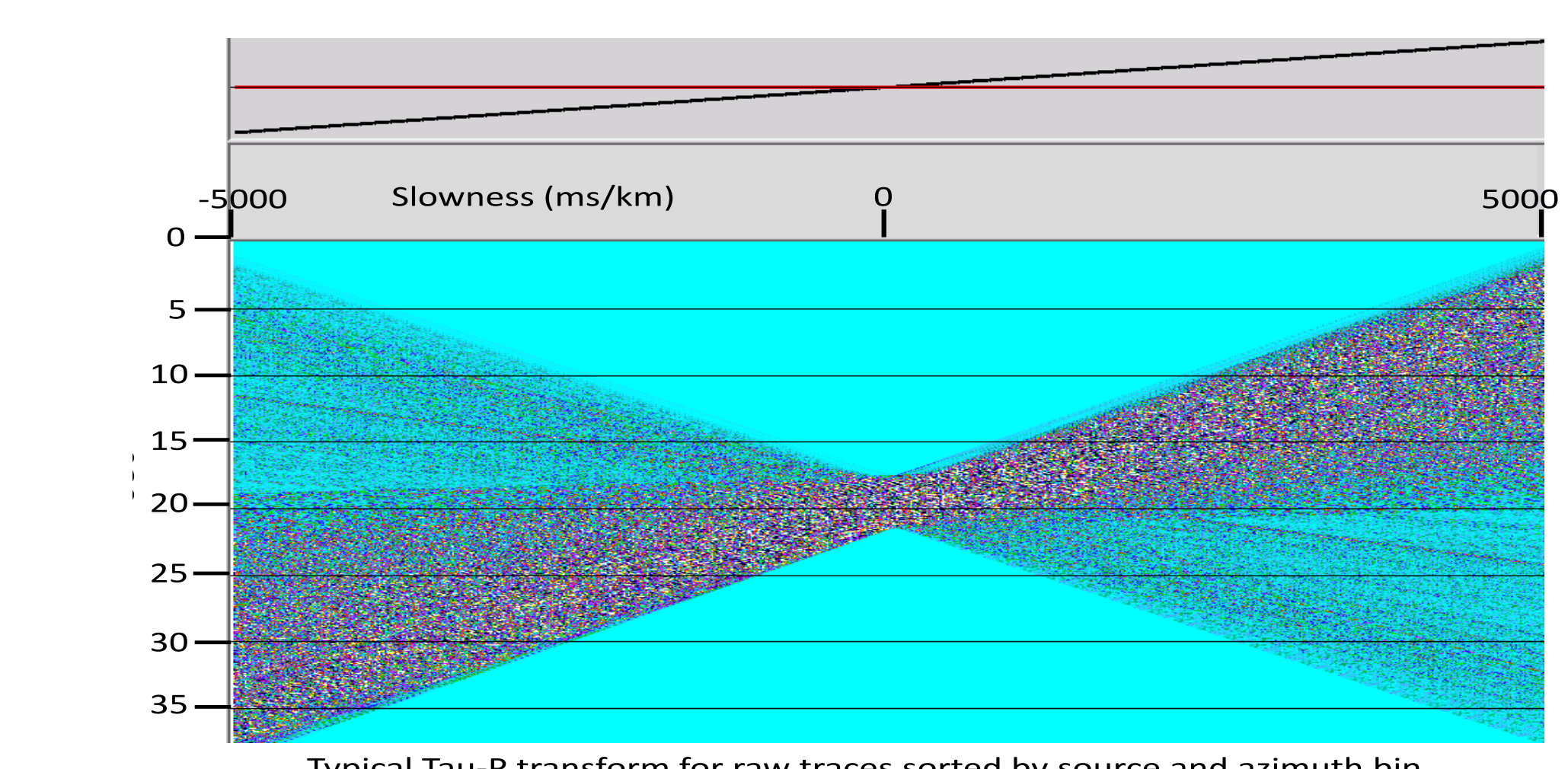


FIG. 11. Tau-P Transform illustrating the massive storage needed.